Asian Journal of Chemistry; Vol. 29, No. 10 (2017), 2184-2190
ASIAN JOURNAL OF CHEMISTRY
https://doi.org/10.14233/ajchem.2017.20677

Crystal Structure and EPR Studies of Potassium Catena-μ-dichromatodiammine cuprate and Dynamic Behaviour of Cu(II) Doped Potassium Catena-μ-dichlorodiammine-cadmium(II)

K. VIJAYARAJ[1], A. JAWAHAR[1], R. ANANTHARAM[2] and M. KUMARA DHAS[3,*]

[1]Department of Chemistry, Nadar Mahajana Sangam S. Vellaichamy Nadar College, Nagamalai, Madurai-625 019, India
[2]Department of Chemistry, Ayya Nadar Janaki Ammal College, Sivakasi-626 123, India
[3]Department of Physics, Mahendra Arts and Science College, Kalippatti, Namakkal-637 501, India

*Corresponding author: E-mail: nmdhas@gmail.com

Received: 29 March 2017; *Accepted*: 30 May 2017; *Published online*: 31 August 2017; AJC-18516

Single crystals of $K_2[Cu(NH_3)_2(CrO_4)_2]$ (PCDCU) and copper(II) doped $K_2[Cd(NH_3)_2(CrO_4)_2]$ (PCDC) have been prepared. $K_2[Cu(NH_3)_2(CrO_4)_2]$ crystallizes in triclinic modification with P1 symmetry, with one formula unit per unit cell. The units are linked to form a polymeric anionic chain, extending along the a axis. The temperature dependence of the EPR spectra of polycrystalline sample of Cu(II) doped $K_2[Cd(NH_3)_2(CrO_4)_2]$ has been studied. The fluxional behaviour of the system is interpreted based on the Boltzmann population of the unpaired electron in the three potential valleys. Though $K_2[Cu(NH_3)_2(CrO_4)_2]$ contains only one CuN_2O_4 octahedron per unit cell, one more signal with low intensity has been observed in the single crystal EPR spectrum.

Keywords: Electron paramagnetic resonance, Dynamic behaviour, Potential valleys.

INTRODUCTION

Octahedral or near octahedral complexes have been subjected to intense investigation, due to their role in understanding the different models of Jahn Teller distortions, *viz.*, dynamic, static and tunneling [1-9]. Most of the copper complexes exhibit tetragonally elongated octahedral geometries, due to J-T vibronic coupling. The compressed geometry observed in a few cases, is in fact, due to the ligand field or steric strain [10]. Intrinsic J-T coupling of Cu^{2+} ion completes with the crystal lattice strain effect and results in dynamic J-T property [10-15]. Temperature dependent EPR spectroscopy has been employed to study such dynamic J-T behaviour [16].

Dynamic J-T effect, called as pseudo J-T effect is observed in Cu^{2+} ions, present in a site of lower symmetry [17,18]. Such dynamic behaviour is explained using different theoretical models. Complexes, reported to have tetragonally compressed geometry and d_z^2 ground state, were found to result from the dynamic equilibrium between the long and intermediate bonds of the tetragonally elongated octahedra with $d_{x^2-y^2}$ ground state, leading to plasticity [14].

Under the fluxional model [2], the observed stereochemistry at a particular temperature is determined by the relative thermal population of the three available potential energy wells. Each of the well corresponds to an elongated octahedron, misaligned in three mutually perpendicular directions. Hopping between these wells leads to dynamic J-T behaviour. For Cu^{2+}, doped into Zn^{2+} Tutton salts with counter cations, other than K^+, the Silver and Getz model gives a poor approximation [15].

In dynamic J-T phenomena, where the Silver and Getz model failed, the RHW model (vibronic coupling model) supplemented it. It was used to calculate the energy states and vibronic wave functions of six coordinate Cu^{2+} complex under the influence of both J-T coupling and lattice strain interactions [19,20]. Calculations were based on atomic displacements, distance between atoms and thermal ellipsoid parameters [21,22]. The temperature dependent ligand field has also been attributed to the g-variation in many complexes [23].

Interest in fluxional behaviour has increased due to the dynamic nature of Cu(II) sites in proteins. Conformational changes were suggested by EPR and Raman spectra [24]. Vibronic interactions were suggested to be responsible for the temperature dependent EPR spectra of blue copper proteins [25]. Further, such studies reveal the low energy pathways involved in chemical reactions [26,27]. The vibronic coupling plays a key role in the mechanism of the behaviour of the "warm" superconductors [28,29].

The first two interactions are based on the electron-nucleus interactions, which introduce the anharmonicity in the potential surfaces. This leads to mean ligand–field strength, which is a function of temperature [30]. While systems containing Cu(II)

dopant showed dynamic J-T behaviour, the corresponding undiluted complexes exhibited strong cooperative phenomena between elongated octahedra. It is interesting to note that the deuteration of $(NH_4)_2[Cu(H_2O)_6(SO_4)_2]$ results in a dynamic behaviour, by interchanging long and intermediate Cu-O bonds [31].

Electron paramagnetic resonance spectra of Cu(II) doped $(NH_4)_2[Zn(NH_3)_2(CrO_4)_2]$ (hereafter referred to as ACDZ) was interpreted to indicate the presence of ground state [32]. The changes in the single crystal EPR at low temperature were deduced to be a phase transition at 278 K. The temperature dependent EPR of $(NH_4)_2[Cd(NH_3)_2(CrO_4)_2]$ (hereafter referred to as ACDC) was attributed to the structural changes due to the reorientation of ammonia molecules [33]. The high and low temperature crystal structures [34] of ACDC revealed a phase transition below 290 K, forming a triclinic lattice, isomorphous with the undiluted copper complex [35].

Generally, the Cu^{2+} ions are used as a probe to enter the lattice substitutionally in place of the divalent cation [36-42]. The EPR studies on Cu^{2+} doped NINS single crystal indicates that the paramagnetic center has a rhombic symmetry with the Cu^{2+} ion having distorted octahedral environment [43]. The electron paramagnetic resonance spectra of Cu^{2+} doped diaqua-*bis*(nicotinamide)*bis*(*o*-sulfobenzimidato-N)-cadmium(II) single crystal shows that the Cu^{2+} ions substitute for magnetically in equivalent Cd^{2+} ions and observed two magnetically in equivalent Cu^{2+}sites [44]. Also, the single crystal EPR spectra at room temperature shows that two different Cu^{2+} complexes were located in different chemical environments which contained two magnetically nonequivalent Cu^{2+} sites [45].

The EPR and optical absorption study of Cu^{2+} doped lithium potassium sulphate single crystals show that the copper enters the lattice substitutionally and is trapped at two magnetically in equivalent sites [46]. Kripal *et al.* [47] reported the EPR and optical absorption studies of copper ions in diglycine calcium chloride tetrahydrate. Recently, Ucar [48] observed the Cu^{2+} and VO^{2+} ion substitute with the Zn^{2+} ion in the host lattice of VO^{2+} and Cu^{2+} doped Zn(II) complex. The angular variations of the EPR spectra shows that two different Cu^{2+} and VO^{2+} complexes are located in different chemical environments and each environment contains two magnetically in equivalent $Cu^{2+}$and VO^{2+} sites in distinct orientations occupying substitutional positions in the lattice and show very high angular dependence.

Behaviour of Cu(II) doped $K_2Mg(H_2O)_6(SO_4)_2$ and the corresponding zinc salts, with other counter cations have been reported to be different [19]. Changes of anions often lead to change of structure and magnetic properties of the Cu(II) octahedra in complexes of the type $Cu(en)_3X_2$, where X = SO_4 or Cl [49]. Studies on Cu(II) doped, $K_2Cd(NH_3)_2(CrO_4)_2$(KCdCr), were under taken with a view to prove into the fluxional behaviour of Cu N_2O_4 chromophore in the light of the J-T behaviour of Cu(II) ion. Possible changes in magnetic and structural properties were analyzed. Further, cooperative phenomena in $KCu(NH_3)_2(CrO_4)_2$, (KCuCr) was investigated using single crystal X-ray diffraction and EPR studies.

As expected, the Cu(II) doped KCdCr reveals dynamic properties, similar to its ammonium analogue. However, the single crystal EPR spectrum of KCuCr exhibits changes, unobserved in the ammonium counterpart.

EXPERIMENTAL

Synthesis of single crystals of $K_2[Cd(NH_3)_2(CrO_4)_2]$ (PCDC) were grown using literature methods, reported for $(NH_4)_2[Cu(NH_3)_2(CrO_4)_2]$ (ACDCU) and $(NH_4)_2[Cd(NH_3)_2(CrO_4)_2]$ (ACDC) respectively [33,35], replacing ammonium dichromate by potassium dichromate. Well developed, dark brown and needle shaped PCDCU and PCDC were obtained. The Cu(II) is doped in PCDC single crystal, yellow prismatic Cu(II) doped crystal were obtained within a week.

X-ray diffraction measurements were carried out on an Enraf-Nonius CAD4 diffractometer, at 293 K. The data were subjected to Lorentz and polarization corrections. All atoms, except hydrogens, were refined anisotropically.

EPR spectra were recorded using a Varian E-112 X-band spectrometer. Elemental analysis was performed, using a GBC 902 atomic absorption spectrometer.

RESULTS AND DISCUSSION

$K_2[Cu(NH_3)_2(CrO_4)_2]$ (PCDCU) crystallizes in the triclinic modification with P1 symmetry, having one formula unit in each unit cell. The crystallographic data are presented in Table-1. The structure of PCDCU is shown in Fig. 1. The bond angles of O–Cu–O and N–Cu–O are in the range of 88-93°, close to the values expected for a regular octahedron. Further, the O–Cr–O angles lie within 106-113°, indicating the tetrahedral nature of CrO_4 units. The Cu–N and Cu–O bond lengths (Table-2) suggest strong Jahn Teller coupling, leading to elongation along Cu–O_2 bond (2.425 Å) while, Cu–O_1 is of intermediate length, the Cu–N_1 is the shortest (1.986 Å). The copper atom is coordinated to four oxygen atoms from CrO_4 units in the equatorial plane and two nitrogen's from two axially disposed ammonia molecules. The units are linked to form a polymeric anionic chain, extending alone the a direction (Fig. 2). While the Cu–N bonds orient along the *c* direction, the Cu-O_4 unit lies in the ab plane, placed in between a and b axes.

TABLE-1
CRYSTALLOGRAPHIC DATA FOR PCDCU AND ACDCU

Empirical formula	$K_2[Cu(NH_3)_2(CrO_4)_2]$	$(NH_4)_2[Cu(NH_3)_2(CrO_4)_2]$
Formula weight	407.54	365.67
Wave length	0.710733 Å	0.71073 Å
Crystal system	Triclinic	Triclinic
Space group	P_1	P_1
Unit all dimensions	a = 8.101(2) Å b = 8.172(2) Å c = 11.9286(11) Å α = 83.482(10)° β = 74.175(11)° γ = 78.28(2)°	a = 7.362(2) Å b = 6.932(1) Å c = 5.895(1) Å α = 112.39(8)° β = 92.79(2)° γ = 107.06(3)°
Volume	744.7(2) $Å^3$	261.5 $Å^3$
Z	1	1
Density calculated	1.836mg/m^3	2.34(5) mg/m^3
F(000)	421	183
Reflections collected	2821	1896
Final R indices	R_1 = 0.0264 WR_2 = 0.0742	0.025
R indices (all data)	R_1 = 0.0278 WR_2 = 0.0759	0.034

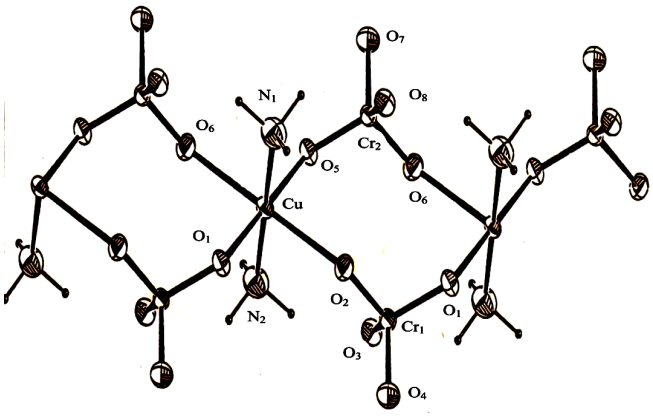

Fig. 1. Ortep diagram of the structure of $K_2Cu(NH_3)_2(CrO_4)_2$ [PCDCU]

TABLE-2
SELECTED INTERATOMIC DISTANCES IN PCDCU (Å)

	Distance		Distance
Cu-N_2	1.957 (0.023)	Cr_1-O_3	1.643 (0.017)
Cu-O_5	1.991 (0.017)	Cr_1-O_1	1.682 (0.018)
Cu-N_1	1.986 (0.018)	Cr_1-O_4	1.674 (0.016)
Cu-O_1	2.049 (0.015)	Cr_2-O_8	1.591 (0.015)
Cu-O_6	2.417 (0.018)	Cr_2O_7	1.652 (0.017)
Cu-O_2	2.425 (0.019)	Cr_2O_6-$\$_2$	1.678 (0.016)
Cr_1-O_2-$\$_2$	1.601 (0.018)	Cr_2O_5	1.698 (0.018)

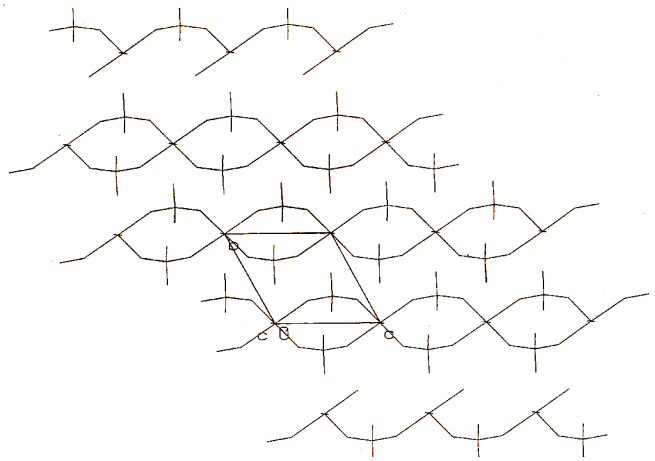

Fig. 2. Line diagram of PCDCU, showing view down *c* axis and extension of chain along a-axis (ortep)

Temperature dependent EPR spectra of polycrystalline sample of Cu(II) doped PCDC, in the range of 77-303 K are shown in Fig. 3. Copper hyperfine features are evident, espe-

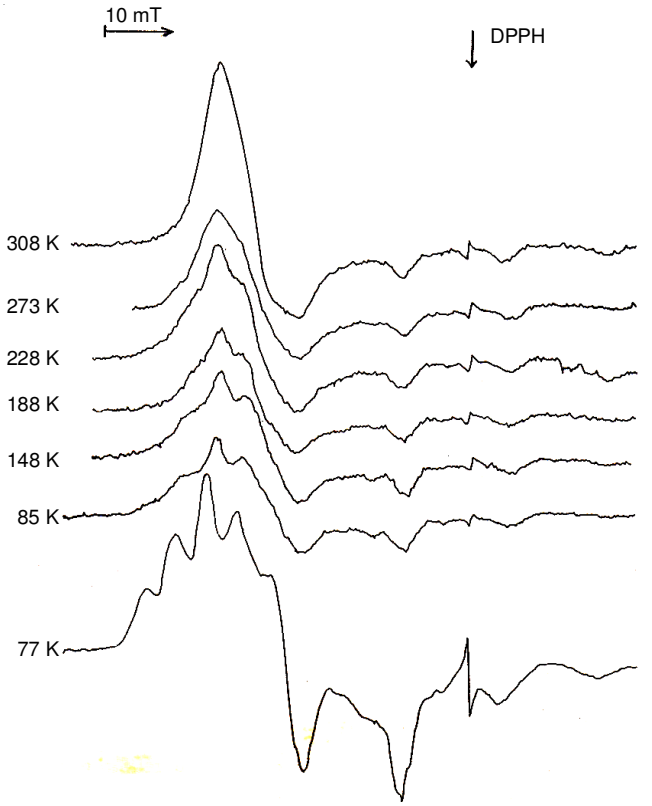

Fig. 3. Temperature dependent EPR spectra of polycrystalline sample of Cu(II) doped PCDC (77 to 300 K)

cially at low temperatures. The apparent ground state at room temperature is d_z^2, as indicated by $g_1 \approx g_2 > g$ (Table-3). The g values compare well with those of Cu(II) in ACDC at 300 and 77 K. With increasing temperature, the highest g factor g_1 decrease while the intermediate one, g_2 increases. The lowest g-tensor, g_3 remains temperature dependent. At 303 K, g_1 and g_2 nearly coalease, leading to axial symmetry. The temperature variation of g-tensor is shown in Fig. 4. The A tensor values, extractable only at low temperature, exhibit a similar trend. However, A_3 is the longest, followed by A_2 and A_1 in that order.

Copper(II) doped $(NH_4)_2[Zn(NH_3)_2(CrO_4)_2]$ (ACDZ) and $(NH_4)_2[Cd(NH_3)_2(CrO_4)_2]$ (ACDC) have shown temperature dependent EPR behaviour [33-35,50], similar to Cu(II) doped PCDC. The two dimensional fluxional behaviour of the CuN_2O_4 chromophore in these systems were interpreted in terms of three in equivalent J-T valleys [50], as well as dynamic vibronic coupling [34]. In the first model, the temperature

TABLE-3
SPIN HAMILTONIAN PARAMETERS FOR Cu(II)/PCDC, PCDCU AND RELATED COMPOUNDS (A, in units of 10^{-4} cm^{-1})

Host lattice	Temp. (K)	g_1	g_2	g_3	A_1	A_2	A_3	Ref.
PCDCU	300	2.2986	2.0951	2.0374	–	–	–	Present work
	77	2.2977	2.0886	2.0391	–	–	–	Present work
Single crystal	300	2.3078	2.0903	2.0380	–	–	–	Present work
Cu(II)/PCDC powder	300	2.259	2.222	2.015	–	–	158.6	Present work
	77	2.297	2.126	2.018	45.8	54.2	146.6	Present work
$(NH_4)_2[Cd(NH_3)_2(CrO_4)_2]$ single crystal	300	2.229	2.215	2.012	–	–	154.3	[50]
	77	–	–	–	–	43.9	149	–
Powder	300	2.244	2.214	2.013	–	–	–	[50]
	77	2.289	2.113	2.019				–
$(NH_4)_2[Cu(NH_3)_2(CrO_4)_2]$	293	2.33	2.08	2.04	–	–	–	[34,50]
	77	2.30	2.13	2.02	–	–	–	[34,50]

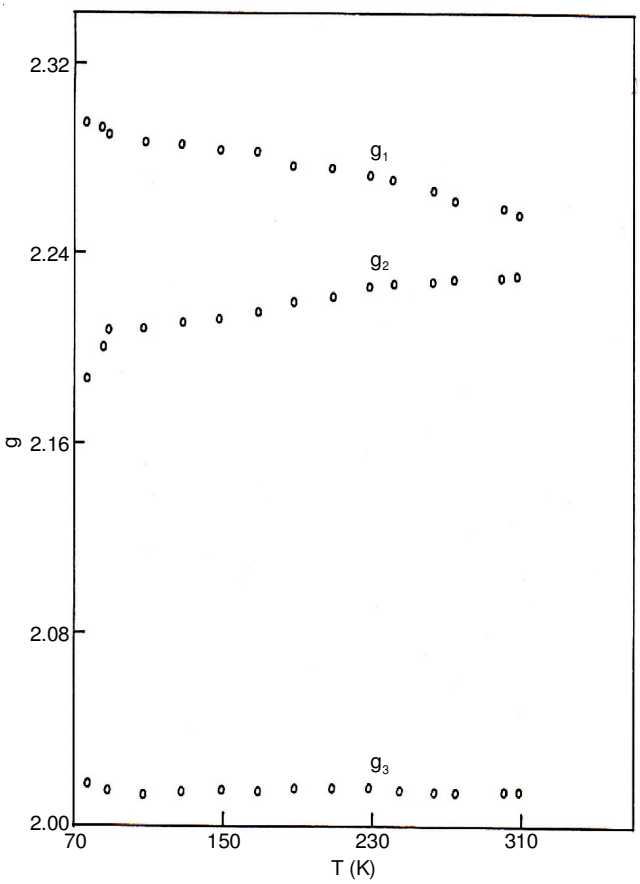

Fig. 4. g-Tensor variation with temperature for Cu(II) doped PCDC

dependent principal g-values and the differences in the energy splitting between the three J-T configurations, the elongation axes of which are misaligned by 90° to each other, were related to the Boltzmann population by the unpaired electron in the three potential valleys.

The model proposed for Cu(II) doped PCDC is illustrated in Fig. 5. The least populated higher energy well 3, corresponds to the configuration with elongation along the short Cu-N bond, which experiences the maximum lattice strain and the g-factor g_1. The most stable well 1 is populated by the structure, elongated along the favoured Cu–O_1 direction and the intermediate well 2 lying closer to well 1, refers to the species with elongation along Cu-O_3 bond. The ground state electronic configuration is $d_{x^2-y^2}$ in all the three configurations. When E < kT, hopping occurs between wells 1 and 2, resulting in fluxionality between Cu-O_1 and Cu-O_3 bonds (and temperature dependence of g_1 and g_2). Since the frequency of hopping is greater than the EPR time scale, an average picture, leading to a compressed geometry is experienced at room temperature. Well 3, being higher in energy, is unaffected by increase of temperature. However, a temperature, as low as 77 K, is not sufficient to freeze the system completely in the lowest valley 1. Assuming Boltzmann distribution and using the Silver and Getz model [2], the relative population, K, calculated at various temperatures, between wells 1 and 2, was employed to arrive at the value of $\delta_{1,2}$, their inter valley energy barrier. The data, listed along with ACDZ, ACDC and Tutton's salts are provided in Table-4. It is interesting to note that the substitution of NH_4^+ ion by K^+ ion decreases the $\delta_{1,2}$ values, a trend observed in

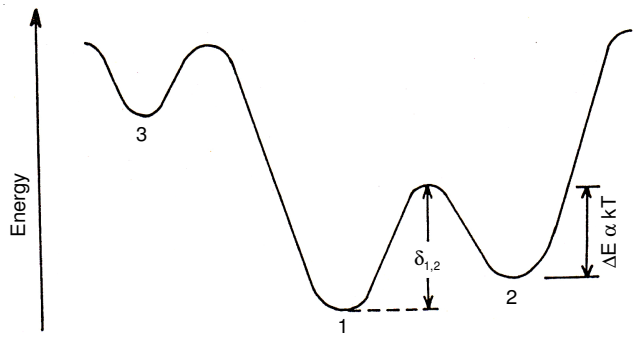

Fig. 5. Potential energy associated with the three elongated CuN_2O_4 octahedra of PCDC. The elongation direction (….) is indicated

TABLE-4
INTER VALLEY ENERGY BARRIER FOR Cu(II) DOPED PCDC

Compound	$\delta_{1,2}$ (cm^{-1})	Ref.
$K_2[Cd(NH_3)_2(CrO_4)_2]$ (PCDC)	127	Present work
$(NH_4)_2[Cd(NH_3)_2(CrO_4)_2]$	190	[29]
$(NH_4)_2[Cd(NH_3)_2(CrO_4)_2]$	230	[29]
$K_2[Mg(H_2O)_6(SO_4)_2]$	90	[31]
$K_2[Zn(H_2O)_6(SO_4)_2]$	75	[29]
$(NH_4)_2[Cd\ Zn(H_2O)_6(SO_4)_2]$	230	[30]
$Rb_2[Zn(H_2O)_6(SO_4)_2]$	175	[30]
$Cs_2[Zn(H_2O)_6(SO_4)_2]$	290	[30]

Tutton's salts [2,51,52]. While ACDC gives a value of 190 cm^{-1} while PCDC yields only 127 cm^{-1}. This lowering could be attributed to the H-bonding network formed by the counter cations NH_4^+, with the oxygens, ligated to copper [35]. The fluxional movement of Cu-O bonds is, thus restricted to hydrogen bonding attraction, resulting in higher $\delta_{1,2}$ for the ammonium analogue.

Fig. 6 presents the X-band powder EPR spectra of PCDCU at 77 K and 300 K, revealing a ground state and a tetragonal elongation with an orthorhombic component. The g-tensor values are provided in Table-3. The g-values compare well with those of ACDCU at 300 and 77 K. Absence of any temperature dependence rules out any dynamic behaviour as witnessed in the doped lattice. Hence, a strong J-T coupling, even at higher temperatures is revealed.

Typical single crystal EPR spectra for the c axis rotation are shown in Fig. 7. Two signals are observed, the g-tensors of which are misaligned by 90°, as indicated by the angular variation of the g-tensors for a*, b* and c* axis rotations (Fig. 8). When the maximum and minimum g-values match with the powder values of g_1 and g_2, the two sets of signals may correspond to two possible orientations of the orthorhombically distorted tetragonally elongated geometry. Of the two orientations, one has elongation along Cu-O_2 and the other along Cu-N. Similar results have been obtained in $[Cu\{P(C_5H_4N)_3\}_2Br_2{\cdot}8H_2O]$ [53]. The intensities of the two signals are obviously different, one of them being very weak, which is due to the species with elongation Cu-N bond.

A similar behaviour has also been noticed in $(NH_4)_2[Cu(NH_3)_2(CrO_4)_2]$ [53]. Although the triclinic unit cell contains only one CuN_2O_4 octahedron, the presence of the second signal with very low intensity could be attributed to the small disorder in the crystal, indicated by the site occupancy factor (sof) for some of the atoms in the octahedron.

Fig. 6. Powder EPR spectra of PCDCU at 77 K and 300 K

Appearance of three such signals has also been explained due to the occurrence of three domains within which the elongated octahedral are in an antiferrodistortive order and the ordered domain extend only for a few adjacent cells [49] for $Cu(en)_3SO_4$. Similar variations in intensities of the two antiferrodistortively coupled octahedral have been revealed by the 4 K spectrum of Cu(II) doped $(3Cl\text{-}en)_8(CDCl_6)Cl_4$ [14].

In contrast to the intensity ratio 1:2 in $(NH_4)_2Cu(NH_3)_2(CrO_4)_2$ [29], the ratio appears to be 1:12. Further, the smaller signal is split into two approximately equal signals in the case of PCDC in certain orientations. This may be due to the appearance of third species, with elongation along the $Cu\text{-}O_1$ direction, which in other orientations, may coincide with the direction Cu-N.

Rotations about the needle and b* axes revealed clearly the presence of again two sites. The g-tensors of the two sites move parallel to each other in these planes, as expected, with nearly the same intensity ratios as in the c axis rotation. The direction cosines obtained from G matrix matches with those from the crystal data. Hence, the principal g-tensors orient along the bond directions.

Conclusion

Crystal structure studies suggest strong J-T coupling in PCDCU, which contains the CrO_4 units, linked to form a polymeric chain along a axis. While the copper doped cadmium analogue shows temperature dependent J-T effect, the undiluted system has no such dynamic behaviour. The presence of a less intense signal in the EPR spectrum of PCDCU is due to the small disorder in the crystal. The Boltzmann population of the unpaired electron is mainly in potential valleys 1 and 2 and the population in well 3 is unaffected by temperature.

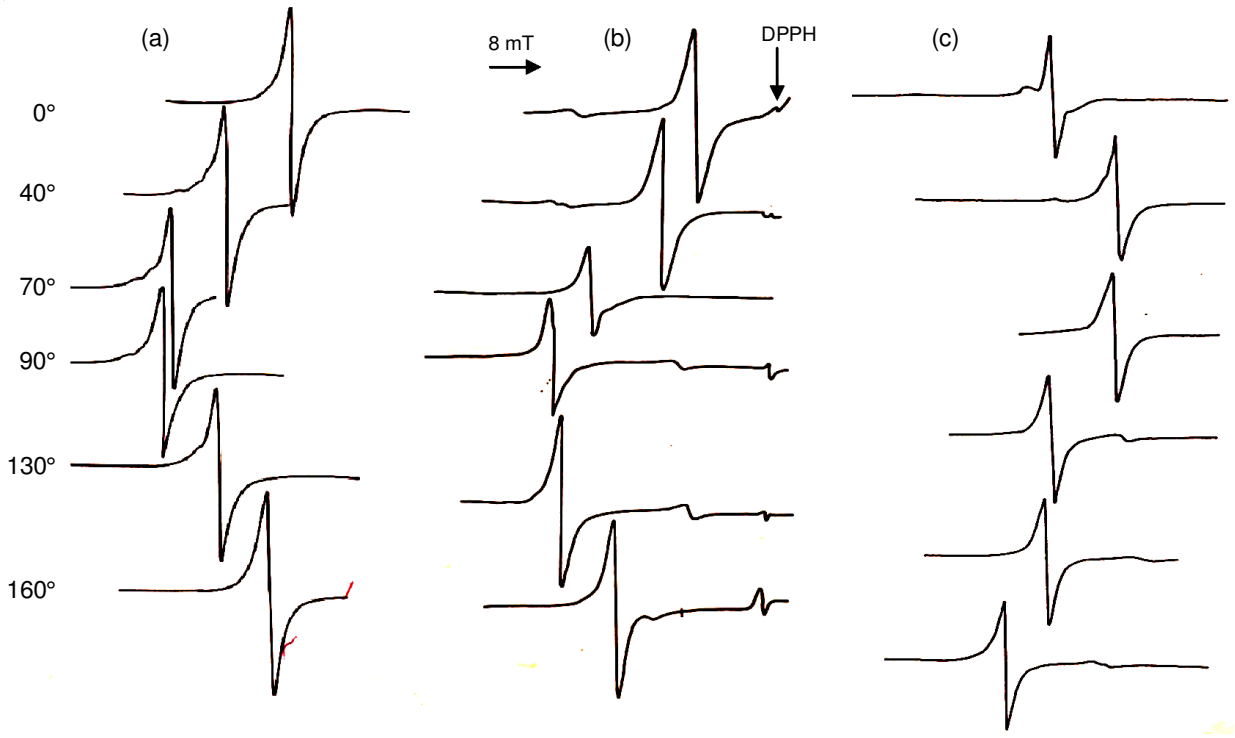

Fig. 7. Angular variation of EPR spectra of PCDCU for axis rotation of (a) a*c* plane, (b) a*b plane and (c) bc*plane

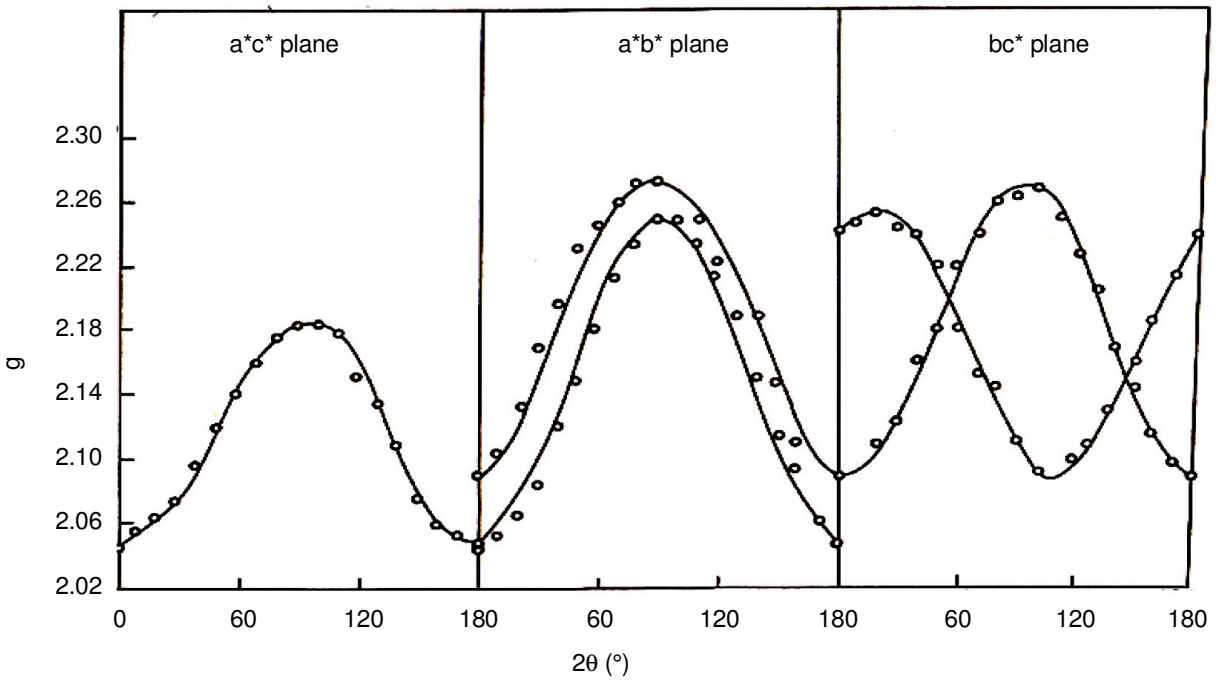

Fig. 8. Angular variation of g-tensors for the three axes

ACKNOWLEDGEMENTS

The authors K. Vijayaraj and A. Jawahar, thank the Management of Nadar Mahajana Sangam S. Vellaichamy Nadar College, Madurai, India for encouragement and permission to carry out this work.

REFERENCES

1. R. Biyik, R. Tapramaz and O.Z. Yesilel, *Spectrochim. Acta A*, **68**, 394 (2007); https://doi.org/10.1016/j.saa.2006.12.008.
2. D. Getz and B.L. Silver, *J. Chem. Phys.*, **61**, 630 (1974); https://doi.org/10.1063/1.1681939.
3. J.S. Wood, C.P. Keijzers, E. De Boer and A. Buttafava, *Inorg. Chem.*, **19**, 2213 (1980); https://doi.org/10.1021/ic50210a004.
4. J. Ammeter, H.B. Buergi, E. Gamp, V. Meyer-Sandrin and W.P. Jensen, *Inorg. Chem.*, **18**, 733 (1979); https://doi.org/10.1021/ic50193a042.
5. R. Kripal, M.P. Yadav and S. Shukla, *Spectrochim. Acta A Mol. Biomol. Spectrosc.*, **78**, 354 (2011); https://doi.org/10.1016/j.saa.2010.10.020.
6. R. Prabakaran, K.J. Sheela, S.M. Rosy, S.R. Krishnan, V.M. Shanmugam and P. Subramanian, *Physica B*, **434**, 155 (2014); https://doi.org/10.1016/j.physb.2013.11.019.
7. I.B. Bersuker, *Coord. Chem. Rev.*, **14**, 357 (1975); https://doi.org/10.1016/S0010-8545(00)80266-0.
8. B. Karabulut, F. Duzgun, C. Keser and Z. Heren, *Physica B*, **396**, 8 (2007); https://doi.org/10.1016/j.physb.2007.01.023.
9. D. Reinen, *Solid State Commun.*, **21**, 137 (1977); https://doi.org/10.1016/0038-1098(77)91496-X.
10. M.J. Riley, M.A. Hitchman, D. Reinen and G. Steffen, *Inrog. Chem.*, **27**, 1924 (1988); https://doi.org/10.1021/ic00284a021.
11. S.K. Hoffmann, J. Goslar and K. Tadyszak, *J. Magn. Reson.*, **205**, 293 (2010); https://doi.org/10.1016/j.jmr.2010.05.014.
12. R. Kripal, S. Shukla and P. Dwivedi, *Physica B*, **407**, 656 (2012); https://doi.org/10.1016/j.physb.2011.11.053.
13. B. Walsh, B.J. Hathaway, *J. Chem. Soc. Dalton Trans.*, 681 (1980); https://doi.org/10.1039/DT9800000681.
14. B. Wagner, S.A. Warda, M.A. Hitchman and D. Reinen, *Inorg. Chem.*, **35**, 3967 (1996); https://doi.org/10.1021/ic951418e.
15. A. Murphy, B.J. Hathaway and T.J. King, *J. Chem. Soc., Dalton Trans.*, 1646 (1979); https://doi.org/10.1039/dt9790001646.
16. E. Poonguzhali, R. Srinivasan, R. Venkatesan, R.V.S.S.N. Ravikumar and P. Sambasiva Rao, *J. Phys. Chem. Solids*, **64**, 1139 (2003); https://doi.org/10.1016/S0022-3697(03)00040-4.
17. S.V. Nistor, M. Stefan, E. Goovaerts, F. Ramaz and B. Briat, *J. Magn. Reson.*, **259**, 87 (2015); https://doi.org/10.1016/j.jmr.2015.07.009.
18. C.V. Reddy, G.V.S.S. Sarma, R.V.S.S.N. Ravikumar and J. Shim, *Optik*, **127**, 4536 (2016); https://doi.org/10.1016/j.ijleo.2016.01.197.
19. M.J. Riley, M.A. Hitchman and A.W. Mohammed, *J. Chem. Phys.*, **87**, 3766 (1987); https://doi.org/10.1063/1.452932.
20. M.J. Riley, M.A. Hitchman and D. Reinen, *Chem. Phys.*, **102**, 11 (1986); https://doi.org/10.1016/0301-0104(86)85113-8.
21. H.B. Burgi, *Trans. Am. Crystallogr. Assoc.*, **20**, 61 (1984).
22. M. Stebler and H.B. Buergi, *J. Am. Chem. Soc.*, **109**, 1395 (1987); https://doi.org/10.1021/ja00239a020.
23. D.K. De, *J. Chem. Phys.*, **79**, 535 (1983); https://doi.org/10.1063/1.445854.
24. D.F. Blair, G.W. Campbell, V. Lum, C.T. Martin, H.B. Gray, B.G. Malmström and S.I. Chan, *J. Inorg. Biochem.*, **19**, 65 (1983); https://doi.org/10.1016/0162-0134(83)85013-2.
25. M. Bacci and S. Cannistraro, *Chem. Phys. Lett.*, **133**, 109 (1987); https://doi.org/10.1016/0009-2614(87)87030-6.
26. J. Gazo, I.B. Bersuker, J. Grej, M. Kabesova, J. Kabout, H. Longfelderova, M. Melmk, M. Serator and F. Velach, *Coord. Chem. Rev.*, **19**, 253 (1976); https://doi.org/10.1016/S0010-8545(00)80317-3.
27. B.J. Hathaway, *Struct. Bonding*, **57**, 55 (1984); https://doi.org/10.1007/BFb0111454.
28. D.V. Fil, O.I. Tokar, A.L. Shelankov and W. Weber, *Phys. Rev. B*, **45**, 5633 (1992); https://doi.org/10.1103/PhysRevB.45.5633.
29. R. Englman, B. Halperin and M. Weger, *Solid State Commun.*, **70**, 57 (1989); https://doi.org/10.1016/0038-1098(89)90467-5.
30. M. Bacci, *Chem. Phys.*, **88**, 39 (1984); https://doi.org/10.1016/0301-0104(84)85101-0.

31. C.J. Simmons, M.A. Hitchman, H. Stratemeier and A.J. Schultz, *J. Am. Chem. Soc.*, **115**, 11304 (1993); https://doi.org/10.1021/ja00077a032.
32. J. Chandrasekaran and S. Subramanian, *J. Magn. Reson.*, **16**, 82 (1974).
33. D.M. Wang, I. Kovacik, E.J. Reijerse and E. de Boer, *J. Chem. Phys.*, **97**, 3897 (1992); https://doi.org/10.1063/1.462928.
34. H. Headlam, M.A. Hitchman, H. Stratemeier, J.M.M. Smits, P.T. Beurskens, E. de Boer, G. Janssen, B.M. Gatehouse, G.B. Deacon, G.N. Ward, M.J. Riley and D. Wang, *Inorg. Chem.*, **34**, 5516 (1995); https://doi.org/10.1021/ic00126a023.
35. B.M. Gatehouse and L.W. Guddat, *Acta Crystallogr.*, **43**, 1445 (1987); https://doi.org/10.1107/S0108270187091492.
36. S. Mukherjee and A.K. Pal, *J. Non-Cryst. Solids*, **341**, 170 (2004); https://doi.org/10.1016/j.jnoncrysol.2004.04.016.
37. R. Kripal and S. Misra, *J. Magn. Magn. Mater.*, **294**, 72 (2005); https://doi.org/10.1016/j.jmmm.2004.12.037.
38. P. Dwivedi, R. Kripal and M.G. Misra, *J. Alloys Comp.*, **499**, 17 (2010); https://doi.org/10.1016/j.jallcom.2010.03.126.
39. S. Boobalan and P. Sambasiva Rao, *J. Phys. Chem. Solids*, **71**, 1527 (2010); https://doi.org/10.1016/j.jpcs.2010.07.019.
40. Y. Celik, E. Bozkurt, I. Ucar and B. Karabulut, *J. Phys. Chem. Solids*, **73**, 1010 (2012); https://doi.org/10.1016/j.jpcs.2012.03.005.
41. A.T. Brant, D.A. Buchanan, J.W. McClory, P.A. Dowben, V.T. Adamiv, Ya.V. Burak and L.E. Halliburton, *J. Lumin.*, **139**, 125 (2013); https://doi.org/10.1016/j.jlumin.2013.02.023.
42. I. Yildirim, B. Karabulut and O. Buyukgungor, *Spectrochim. Acta A*, **152**, 608 (2016); https://doi.org/10.1016/j.saa.2015.01.100.
43. I. Uçar, N. Dege, B. Karabulut and A. Bulut, *J. Phys. Chem. Solids*, **68**, 1540 (2007); https://doi.org/10.1016/j.jpcs.2007.03.033.
44. E. Bozkurt and B. Karabulut, *Spectrochim. Acta A*, **73**, 871 (2009); https://doi.org/10.1016/j.saa.2009.04.015.
45. M. Fidan, F. Semerci, E. Sahin, O.Z. Yesilel, R. Tapramaz and Y. Sahin, *Spectrochim. Acta A*, **110**, 437 (2013); https://doi.org/10.1016/j.saa.2013.02.013.
46. R. Kripal, M. Bajpai, M. Maurya and H. Govind, *Physica B*, **403**, 3693 (2008); https://doi.org/10.1016/j.physb.2008.06.019.
47. R. Kripal and M. Bajpai, *Spectrochim. Acta A*, **72**, 528 (2009); https://doi.org/10.1016/j.saa.2008.10.037.
48. I. Ucar, *Spectrochim. Acta A*, **72**, 399 (2009); https://doi.org/10.1016/j.saa.2008.10.013.
49. I. Bertini, P. Dapporto, D. Gatteschi and A. Scozzafava , *J. Chem. Soc. Dalton Trans.*, 1410 (1979); https://doi.org/10.1039/DT9790001409.
50. R. Murugesan, A. Thamaraichelvan, A.M. Franklin and V. Ramakrishnan, *Mol. Phys.*, **79**, 663 (1993); https://doi.org/10.1080/00268979300101521.
51. V.E. Petrashen, Yu.V. Yablokov and R.L. Davidovich, *Phys. Status Solidi B*, **88**, 439 (1978); https://doi.org/10.1002/pssb.2220880208.
52. P.S. Rao, A.K. Viswanath and S. Subramanian, *Spectrochim. Acta A*, **48**, 1745 (1992); https://doi.org/10.1016/0584-8539(92)80248-U.
53. T. Astley, H. Headlam, M.A. Hitchman, F.R. Keene, J. Pilbrow, H. Stratemeier, E.R.T. Tiekink and Y.C. Zhong, *J. Chem. Soc., Dalton Trans.*, 3809 (1995); https://doi.org/10.1039/DT9950003809.